

Dedicated to Prof. Dorin N. Poenaru's
70th Anniversary

TOTAL ABSORPTION PECTROSCOPY

B. RUBIO¹, W. GELLETLY²

¹IFIC, CSIC-Un. Valencia, Ap. 22085, ES-46071 Valencia, Spain

E-mail: Berta.Rubio@ific.uv.es

² Physics Department, University of Surrey

E-mail: W.Gelletly@surrey.ac.uk

(Received February 22, 2007)

Abstract. The problem of determining the distribution of beta decay strength ($B(\text{GT})$) as a function of excitation energy in the daughter nucleus is discussed. Total Absorption Spectroscopy is shown to provide a way of determining the $B(\text{GT})$ precisely. A brief history of such measurements and a discussion of the advantages and disadvantages of this technique, is followed by examples of two recent studies using the technique.

Key words: beta decay, $B(\text{GT})$, mass separators, total absorption spectroscopy.

1. INTRODUCTION

Our present knowledge of atomic nuclei suggests that some 6 000–7 000 distinct nuclear species live long enough to be created and studied. These limits are set by the proton- and neutron- drip-lines in terms of how many protons (neutrons) the nuclear ground state can hold and still be bound, and by the heaviest elements that can exist [1]. Figure 1 summarises this in the form of the chart of the nuclides, where we see the drip-lines suggested by our knowledge of nuclear masses and the, as yet undefined, limit in terms of the highest proton number (Z) we can reach.

Figure 1 also summarises much of our knowledge of nuclei. We see the stable nuclei, the filled black squares, initially stretching along the $N = Z$ line but then moving steadily to the neutron-rich side of the chart because of the increasingly disruptive effect of the Coulomb force.

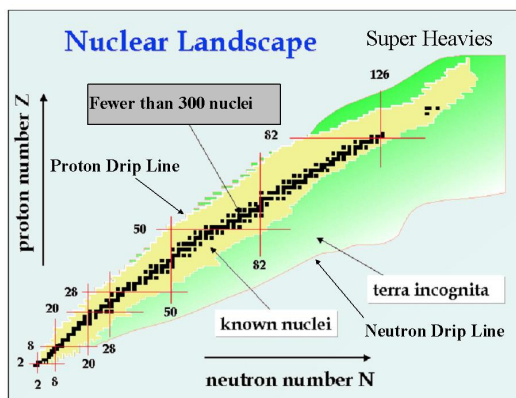


Fig. 1 – The chart of the nuclides.

In essence we have two main ways of studying nuclear properties, namely in reactions and in radioactive decay. The former has the attraction of flexibility and versatility since it allows us to vary the angular momentum and excitation energy in the nuclear system created in the reaction. The latter is inflexible, since nuclear decay is essentially God-given and can only be altered under certain, unusual conditions [2, 3]. Thus radioactive decay is more limited as a tool for studying nuclei but it is often the first means of identifying a new nuclear species and hence also the first harbinger of a knowledge of its properties. If separated from other species present during its production it can also be studied with only a very small number of atoms.

This sensitivity also means that it is a prolific source of applications, a forensic tool that scientists have used in a wide variety of contexts. Examination of Fig. 1 shows us that studies of radioactive decay can provide information about nuclear properties over a wide range of N and Z . Most of the decays are due to beta decay, either β^- decay on the n-rich side of stability or β^+ /EC decay on the p-rich side. At and near the proton drip-line proton decay is also important and as we gradually establish the means to study more and more neutron-rich nuclei we may encounter neutron-decay near the neutron drip-line [4]. In heavy elements alpha decay and spontaneous fission also compete with beta decay. However, overall, beta decay is the most common mode of radioactive decay. The study of beta decay is the subject of this article and we now turn our attention to this topic.

2. BETA DECAY AND NUCLEAR STRUCTURE

One advantage of studying beta decay is that we now have a good understanding of the process. It was not always so. In spectroscopic terms beta

decay was difficult to understand initially because of the continuous nature of the beta spectrum, which is in stark contrast with the discrete line spectra of alpha- and gamma-decay. These are readily understood in terms of transitions between quantum states in nuclei. Pauli's explanation [5] in terms of the neutrino and hence a three-body process clarified this. Soon afterwards, the present basis of our understanding was laid by Fermi's theory of beta decay [6].

Here we are concerned not with the history of the subject but with the use of beta decay as a tool to understand nuclear structure. In particular the question of how we can use beta-decay transition probabilities since they are sensitive to the details of nuclear structure. This is possible if we use the Fermi theory and take into account effects such as the density of states available to the betas and neutrinos in the decay and the Coulomb field felt by the beta particles. From the transition probabilities we can isolate the part relevant to nuclear structure, namely the matrix elements. It turns out, however, that the transition probabilities are not easy to measure, again partly because of the continuous nature of the spectrum and partly because the alternative methods of measurement also present their own difficulties as we will discuss below. This article is concerned particularly with one approach to overcoming these difficulties, namely the method of Total Absorption Spectroscopy.

At first sight one might hazard a guess that such measurements are best done in nuclei close to the line of stability, where the Q -value ($Q = M_{parent} - M_{daughter}$) is small and the number of states populated is limited because of the low level density. Such cases are indeed relatively simple. However the fact that the energy window accessible in such decays is limited restricts its use as a spectroscopic tool. It also turns out that, in general, the more interesting cases to study lie farther from stability. They are the so-called *Allowed decays* where the well-understood properties of the τ (Fermi) and σ (Gamow-Teller) operators apply.

In terms of the isospin formalism, where states are characterised by the quantum numbers T and its third component T_Z , the only unhindered, allowed Fermi decays are the so-called super-allowed decays, those with $\Delta T = 0$. In other words only T_Z changes. Such transitions can only occur when the IAS (Isobaric Analogue State) of the parent state in the daughter nucleus lies within the Q_β window.

As one can see in the typical examples of β^+ and β^- decay shown in Fig. 2, there is another consideration regarding the Fermi transitions. In the β^+ decays of $N > Z$ nuclei the absolute value of T_Z always increases by one unit, consequently it is impossible to keep the T quantum number unaltered unless one is at negative values of T_Z . Thus Fermi decays in nuclei decaying by β^+ emission are very often forbidden. If we again look at Fig. 2 we see that this is not a problem in the nuclei unstable to β^- emission. Here, however,

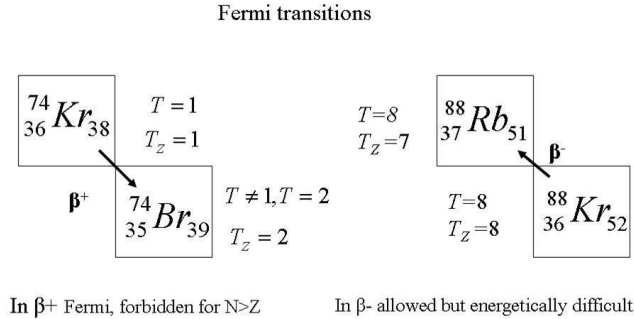


Fig. 2 – Examples of typical beta decays involving electron and positron emission.

since the final states usually have T values one unit higher than the g.s., the IAS is, in general, at high excitation energy and consequently outside the Q_β window. The reader should note that we have assumed here that the ground state and low-lying levels in the nucleus have the lowest isospin possible. This is, in general, a good assumption apart from the nuclei near $N = Z$.

Turning to Gamow-Teller transitions we face a different situation. As for Fermi transitions one can imagine that the operator transforms a neutron to a proton or vice-versa but at the same time the nucleon can have its spin “flipped”. If nuclear forces were spin-independent as well as charge independent we would have a very similar situation to the Fermi decays with the transitions going to the isobaric analogue states. However nuclear forces are strongly spin dependent, as is evidenced from the success of the Shell Model. As a result the states are mixed into nuclear states over a wide range of energy centred at the energy of the expected “resonance” state. Moreover we know now that the residual nucleon-nucleon interaction, and more particularly the $\sigma\sigma\tau\tau$ term, because of its repulsive character, moves the strength from the few MeV, zeroth-order excitation energy of the daughter particle-hole excitations to a resonance peak at typically 15 to 20 MeV excitation and consequently outside the Q_β window. As in the case of the Fermi transitions, there is a difference between the beta-minus and beta-plus decays. In general all that we have said above applies to the beta-minus case but the beta-plus transitions are either very suppressed or forbidden. This is because the allowed orbitals are often occupied on the neutron side. As we shall see later this is not always the case. For instance some times a transition between a state involving a proton with high orbital angular momentum can proceed to the spin-orbit partner state on the neutron side ($J \uparrow \rightarrow J \downarrow$).

All of this may be summarised briefly. Near the line of stability decay schemes are simpler and more amenable to study but, of necessity, carry less

information. Our main aim must be to study transition probabilities in beta decays far from stability where the Q values are large and we have better access to a large fraction of the GT strength. Although we have been studying beta decay for a long time we have only really scratched the surface in terms of studying exotic nuclei. For a variety of reasons experimenters have not devoted the same effort to developing instrumentation for such studies as they have to developing Si and Ge detector arrays for use in studying prompt radiation from reactions. As a result only a limited number of cases has been studied in detail but they reveal what one might expect to learn in the future. Some good examples are the studies of allowed decays to the GT resonance in nuclei: a) just below ^{100}Sn [7] and b) in the rare-earth region [8–12], measurements in $A \sim 70\text{--}80$ nuclei that have allowed the shapes of the parent ground state to be deduced [12,13] or measurements of super-allowed Fermi decays of importance as a test of our understanding of the Weak Interaction [14–16].

3. MEASURING BETA DECAY TRANSITION PROBABILITIES

It is worth reminding the reader of the following relations between a number of quantities:

a) the relationship between the transition probability B_{GT} in natural units and the strength function S_β

$$S_\beta = \frac{1}{6147 \pm 7} \left(\frac{g_A}{g_V} \right)^2 \sum_{E_f \in \Delta E} \frac{1}{\Delta E} B(\text{GT})_{i \rightarrow f}, \quad (1)$$

where g_A and g_V are the Weak Interaction vector and axial-vector coupling constants;

b) the relationship between S_β and the quantities observed in experiment

$$S_\beta = \frac{I_\beta(E)}{f(Q_\beta - E)T_{1/2}}, \quad (2)$$

where I_β is the direct beta feeding to a state of energy E , f (which depends on the Q -value) is the Fermi function and $T_{1/2}$ is the beta decay half life of the parent nucleus. From (2), if we remember the dependence of the Fermi function with the energy, one can see that even a small amount of feeding at high excitation energy close to the Q value will carry a significant part of the strength.

With this in mind, what are the measurements we would like to make on the beta decays of exotic nuclei? Many types of measurement are of interest; too many for us to pursue. Here we will concentrate on the measurement

of the GT reduced transition probability B_{GT} as a function of the excitation energy in the daughter (final) nucleus. At first sight this seems straightforward, one has to measure the beta decay to each individual state (assuming Q_β and $T_{1/2}$ are known), but the beta spectra are continuous and in complex decay schemes difficult to disentangle. As a result one cannot derive the beta feeding to individual states in the daughter nucleus from measurements of the beta particles themselves except in a few simple cases.

How then are the measurements made? If we ignore decays very far from stability, where some of the levels fed in the decay lie above the particle separation energy and hence decay by emitting a particle, the levels that are fed usually decay by electromagnetic transitions. We can then deduce the beta feeding from the difference between the gamma-intensity feeding the level and that de-exciting it with suitable corrections for internal conversion or internal pair production etc. This seems quite simple; it turns out to be fraught with difficulty. Figure 3 illustrates part of the problem. Here we see a typical level

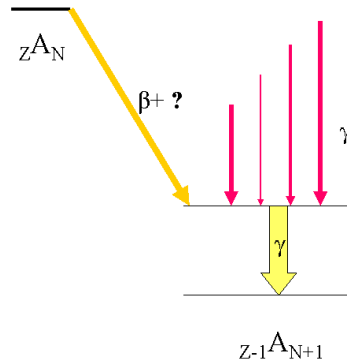


Fig. 3 – The feeding of a typical level in the daughter nucleus in beta decay (see text).

in the daughter nucleus. It is fed directly in beta decay and it is fed indirectly by electromagnetic transitions from higher lying levels. In most experiments the gamma rays are detected using Ge semiconductor detectors, which have moderately good energy resolution and modest efficiencies. At present even the best arrays of such detectors have efficiencies of about 20% for gamma-rays of 1332 keV energy [17]. To make matters worse their detection efficiency is strongly dependent on energy.

If the beta feeding to a level is deduced from the difference between the gamma-ray strength feeding the level and the strength de-populating it and many weak transitions are unobserved then their strength can add up to a sufficiently large number that we get quite the wrong number for the beta

feeding. Thus, if we use detection techniques where the detection efficiency is much less than one, we cannot reliably extract the beta feeding or ft values (the inverse of S_β for a particular level) simply from the gamma-ray balances. As we move away from stability and Q -values increase one expects greater fragmentation of the beta feeding because of the rapid increase in level density with excitation energy. One consequence is that, in general, the average gamma-ray intensity will also be reduced and more gamma rays will not be observed. In addition there will be more feeding of levels at higher energies, which will be de-excited by higher energy gamma rays on average for which the detection efficiency is lower. Thus we can expect this problem to get worse. This problem was recognised some time ago [18] and was named the Pandemonium effect by Hardy *et al.* after the city of Lucifer in Milton's epic poem Paradise Lost, a place where one might expect chaos to reign.

Can this problem be overcome? One solution is to adopt a quite different approach to the measurements. Total Absorption Spectroscopy offers just such an approach. In this method one still detects the secondary gamma rays but one aims to measure the population of the levels directly rather than indirectly as described above. In the ideal case Total Absorption Spectroscopy involves a gamma-ray detector with 100% detection efficiency. In the spectrum from such a detector one will detect for each and every beta decay the summed energy of all the gamma rays in the resulting cascade de-exciting the level that is fed initially. In the section which follows we will look at how this technique has developed over the years. It will be readily obvious that the main difficulty in applying the technique is the creation of a spectrometer with 100% detection efficiency.

An obvious question is "If it is important to obtain reliable and accurate beta strength distributions and Total Absorption Spectroscopy provides the remedy to the problem outlined above, why is it not in widespread use?" The answer lies partly in the difficulty of making a spectrometer with sufficiently high efficiency, partly in the complexity of the analysis of the data collected in such experiments and partly the lack of a detailed study of the assumptions underlying the analysis methods and the associated systematic errors. As we will find out in the next section both of these questions have been addressed.

3.1. A SHORT HISTORY OF TOTAL ABSORPTION SPECTROMETERS

In this section we will look at how the technique of Total Absorption Spectroscopy has developed. Surveys of beta strength functions for significant numbers of unstable nuclei were carried out in the early 1970s at both

ISOLDE [19] and OSIRIS [20]. In these measurements the spectrometer consisted of two cylindrical NaI detectors of 15 cm diameter and 10 cm length. The radioactive source was positioned on the central axis between the two counters. The authors of these two papers describe their method as “incomplete total absorption”, an accurate description given the detection efficiency of the system, which was well short of the ideal outlined above. They took great care in the analysis and they pointed out the inherent difficulties of the analysis of the data. This is not a trivial task as we shall see later. They also used Monte Carlo simulations to construct the response function of the detector. This strikes a chord with current practice as we shall see.

In their introduction of the fictitious nucleus Pandemonium Hardy *et al.* exposed the difficulties in measuring beta strength functions. Stimulated by this and Firestone’s [21] high-resolution studies, Alkhazov [22] measured a number of beta strength functions using a larger NaI detector of dimensions 20 cm diameter by 20 cm length with a well of 4 cm \times 10 cm set into it with the source placed in the well. This system we will call the Russian TAGS. These measurements reinforced the view of Hardy *et al.* that most of the decay schemes in the literature were substantially incomplete and one could not rely on the log ft values derived from them. Clearly a better detection efficiency was the way forward and this came from Greenwood *et al.* [23] who introduced a large, 25.4 cm \times 30.5 cm NaI well counter, and used it to measure beta strength functions for a range of separated fission fragments. This TAGS was a much better approximation to the ideal spectrometer. Again these authors were painstaking in their methods of analysis, which was now based on the simulation of the entire decay scheme using Monte Carlo methods. They too recognised and discussed many of the inherent difficulties in the analysis of the data from such measurements. The beta decays they studied were of particular significance in that the beta decay of fission fragments accounts for some 7% or so of the total heating in a typical operating nuclear reactor and, of necessity, 100% of the heating once the reactor shuts down. For safety and shielding purposes it is thus important to have a good measure of the beta feeding for all these decays so that one can calculate the residual heating of the fuel as a function of time after shutdown.

3.2. MODERN TOTAL ABSORPTION SPECTROMETERS

More recently two larger spectrometers, both with higher detection efficiency, have been deployed to measure beta strength functions. In addition the analysis methods have been optimised after being studied in detail [24]. It is not our purpose here to discuss every aspect of total absorption spectroscopy. We should however remind our reader that the relationship between the beta

feeding $I(E_j)$ and the data d_i measured in channel i in the total absorption spectrometer is given by

$$d_i = \sum_{j=1}^{j_{max}} R_{ij} I_j, \quad (3)$$

where R_{ij} , the response function, is the probability that feeding at an energy E_j produces a count in channel i . In order to determine the response function we need to know how the spectrometer responds to individual quanta and betas as a function of energy and also have a knowledge of the branching ratios for the electromagnetic transitions de-exciting the levels [25]. From Eq. (3) we see that if we want to determine the beta feeding we must solve this inverse problem. This is not trivial because Eq. (3) falls into the class of so-called ‘‘ill-posed’’ problems and their solution is neither trivial nor straightforward. Tain and Cano-Ott [24, 26] have devoted considerable effort to examining how to optimise the solutions and make recommendations on how the analysis should be carried out. For details the reader is referred to their papers. In a nutshell they examined the suitability of three different de-convolution algorithms for extracting the correct intensity distribution from the data.

A knowledge of the branching ratios implies that we know the level scheme, which is often not true. Tain and Cano-Ott also examined how much the results of the analysis depended on assumptions about the branching ratios and were able to show that in the cases they studied the results are insensitive to the initial assumptions. However in other cases [27] it is important to have a solid knowledge of the level scheme. In recent years considerable progress has been made in the Monte Carlo simulation of the response to individual single quanta and this is also an ingredient in the analysis procedure developed by Tain and Cano-Ott. Taken overall these authors have put the analysis of TAgS data on a sound footing although the methods must be applied with due care and attention to the individual case under study.

The most successful TAgS [GSI TAS] built to date was installed at the GSI on-line mass separator [28]. It involved an even larger single NaI detector than that available to Greenwood *et al.*; again it is of cylindrical shape with dimensions 35.6 cm \times 35.6 cm, with a central well which could be filled with a matching plug of NaI. The activity from the mass separator was implanted on to a magnetic tape which was used to carry it to the centre of the crystal. The set up included a small Ge detector and ancillary Si detectors placed inside the well, close to the source position, to allow coincidence measurements of gammas in the large NaI with X-rays and betas or alphas respectively. A whole series of measurements have been made with this device including measurements of the beta decays of spherical, rare-earth nuclei [7–11] and neutron-deficient nuclei just below ^{100}Sn [7]. In addition to their work on the

solution of the “inverse, ill-posed” problem the Valencia group looked at the effect of the non-linearity of the light output in the NaI scintillator [29] and of the pile up in the electronic circuitry [30] and showed that these effects could be taken into account satisfactorily.

More recently the present authors were involved in building and installing a new total absorption spectrometer *Lucrecia* at the CERN-ISOLDE mass separator. There were two main aims for the use of this spectrometer. Firstly to take advantage of the wide range of separated nuclear species available from the ISOLDE separators and secondly to be able to arrange that the separated activity can be deposited directly at the centre of the spectrometer, thus eliminating the delay in carrying the sources from an external point of implantation into the spectrometer. In this mode the tape is used to carry away the daughter activities rather than to refresh the sources under study. The system was designed in such a way that it could still be operated as at GSI with the sources implanted externally then carried to the counting position in the centre of the detector. The *Lucrecia* spectrometer consists of an even bigger single crystal of NaI (38 cm \times 38 cm) with a 7.5 cm through hole, symmetrically placed, at right angles to the axis of the cylinder. From one side the tape and the beam, depending on the half life of interest, enter the crystal. From the other a number of ancillary detectors can be placed close to the counting position so that one can measure the TAgS spectrum in coincidence with electrons, positrons, X-rays and Γ -rays.

In the experiments with this spectrometer described below this involved a 2 mm thick plastic detector for betas placed close to the source and a Ge telescope, consisting of a 1 cm thick planar detector backed by a 5 cm thick co-axial Ge detector.

Detectors as large as the GSI TAS and *Lucrecia* are clearly a much better approximation to the ideal detector than those used earlier. This certainly reduces the uncertainties in the analysis. However it also means that they are more efficient in terms of detecting background radiation. In both cases an effort has been made to minimise the background and improve the sensitivity. At ISOLDE, where the activities are produced in the fission or fragmentation of heavy targets with a beam of 1.4 GeV protons from the PS-Booster, one might expect a significant background from both gamma-rays and neutrons in the experimental hall. To minimise the background overall the spectrometer system was placed inside an 11 ton shield, made up of successive layers of boron-loaded polyethylene(10 cm thick), lead(5.1 cm), copper(1.5 cm) and aluminium(2 cm). The resulting spectra show that this is effective with the main background being due to ^{40}K , which is present as a natural contaminant in the crystal.

Figure 4 makes a comparison of the performance of the two detector systems. On the left it shows views of the two central NaI detectors. The

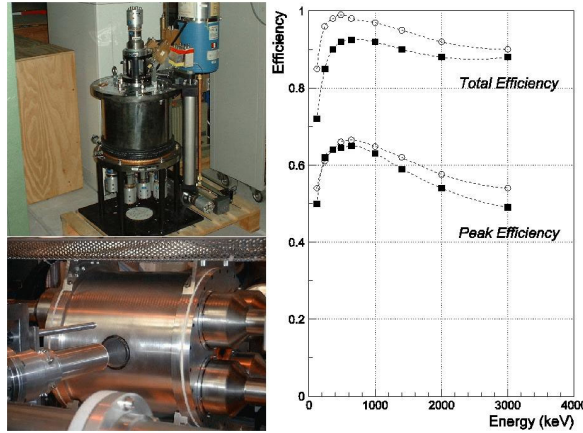


Fig. 4 – On the left we see photographs of the GSI TAS and *Lucrecia*. On the right we see the corresponding total and photopeak efficiency curves for these two detectors. The empty and filled points represent the results for the GSI TAS and *Lucrecia* respectively.

GSI TAS was mounted with the central axis in the vertical direction. *Lucrecia* on the other hand is mounted horizontally, with the through hole pointing along the beamline delivering the radioactive sources. In the photograph we see the through hole with the Ge telescope withdrawn from it on the far side from where the beam enters. On the right of Fig. 4 we see the total and photo-peak efficiencies for the two spectrometers. The empty and filled points represent the results for the GSI TAS and *Lucrecia* respectively. The latter is the larger of the two detectors and instinctively one feels it should have the higher efficiency but one must remember that it was designed to allow the radioactive beam to enter directly and a through hole was used to allow the insertion of the ancillary detectors. In addition, although a matching plug detector is available to fill the hole, it is not used in general in the case of *Lucrecia* since the space is used for the beta and gamma detectors. As a result of the larger volume devoted to the holes penetrating the crystal its efficiency is lower than that of the GSI TAS. In particular the efficiency for detecting a single gamma-ray is lower at all energies. In practice few gamma-ray cascades involve a single gamma ray and so the difference in total efficiency is less dramatic than this. In other respects the two spectrometers are comparable with the energy resolutions and backgrounds being very similar.

4. RECENT MEASUREMENTS

In this section we will discuss the results of two sets of measurements; one carried out with the GSI TAS and the other with *Lucrecia*. They illustrate the

power of the method and part of what it can contribute to our understanding of nuclear structure. One or both of the present authors was(were) involved in these experiments.

4.1. THE GT RESONANCE OBSERVED IN THE DECAY OF ^{150}Ho

This experimental investigation illustrates very well many of the features of beta decay studies we have described above. It not only shows the GT resonance very clearly within the beta window but also shows why one should study beta decay with both the TAgS technique and in high resolution. Figure 5 gives a schematic view of the single particle orbitals available above the ^{146}Gd double-closed shell, or at least those that are relevant to the present discussion. The ^{150}Ho nucleus has two, low-lying, beta-decaying states with spins and parities 2^- and 9^+ respectively. Figure 5 shows the expected configuration of the 2^- isomer with the odd neutron in the $f_{7/2}$ shell and a proton in the $d_{3/2}$ orbit. The reader should remember that the pairs of protons shown in the picture in the $h_{11/2}$ orbit coupled to 0^+ , can scatter between all three orbits ($s_{1/2}$, $h_{11/2}$ and $d_{3/2}$).

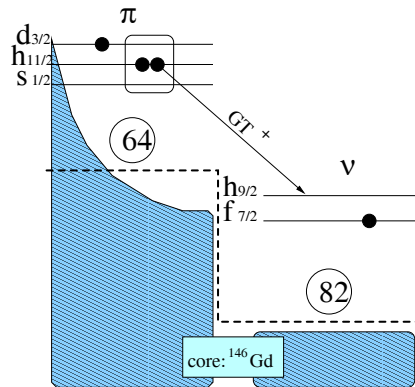


Fig. 5 – A schematic view of the single particle orbitals available above the ^{146}Gd doubly closed shell relevant to the present discussion.

One reason for the interest in this case and in the decays of neighbouring nuclei is that, unusually, most of the GT strength lies within the Q_β window. It is not a very common situation in β^+ decay, as we have explained above, and, in this case, it occurs because the proton is transformed in the transition into a neutron in the spin-orbit partner orbital, which lies within the window. Here the transition is from $\pi h_{11/2}$ to $\nu h_{9/2}$ since the decay of the unpaired proton (in the $d_{3/2}$ orbit) is forbidden. A similar case open to study is the $\pi g_{9/2}$ to $\nu g_{7/2}$ transition which occurs in the $N \sim Z$ nuclei close to ^{100}Sn .

The four-particle states with spins 1^- , 2^- and 3^- populated in the ^{150}Dy daughter nucleus have the configuration $[(\pi d_{3/2} \nu f_{7/2}) (\pi h_{11/2} \nu h_{9/2})]$. A simple approximation to the excitation energy of these states is just twice the pairing gap for protons plus twice the pairing gap for neutrons plus the neutron $h_{9/2}$ single particle energy, i.e. at ~ 5 MeV excitation energy. This is well within the Q_β window of ~ 7 MeV for this decay. It should be noted that this decay is closely connected to the decay of ^{148}Dy , a simpler case since it has just the single proton pair outside the ^{146}Gd core. The two cases must clearly be much the same and should have a comparable log ft namely 3.95(3) [8]. It will, of course, be slightly different because of the presence of the $d_{3/2}$ proton which will modify the probability of the proton pair occupying the $\pi h_{11/2}$ orbital. With this slight caveat we can say that we expect the ^{150}Ho 2^- state to decay strongly to levels at ~ 5 MeV with a log ft of about 3.9.

An important feature of this work is that it has been studied in detail in two ways, with the GSI TAS described earlier and with a highly efficient Ge array called the “CLUSTER CUBE”. This array consisted of six EUROBALL cluster detectors [31] in a highly compact geometry, with four of the detectors 10.2 cm from the source and the other two at a distance of 11.3 cm. The photopeak efficiency of the array at 1332 keV was 10.2(0.5)%. As we shall see this means that one can compare the two methods directly. Because the direct production of ^{150}Ho in a heavy ion reaction would inevitably favour the 9^+ isomeric state, the 2^- state was produced as the daughter activity of ^{150}Er . This results in clean production of the ^{150}Ho via the decay of the 0^+ ground state of ^{150}Er to 1^+ states in ^{150}Ho which decay to the 2^- ground state. The details can be found in refs. [8–10]. Our concern here is with the results.

In Fig. 6 we see the measured beta strength as a function of excitation energy derived from measurements both with the GSI TAS and CLUSTER CUBE. To give our reader a feeling for the quality of the CLUSTER CUBE

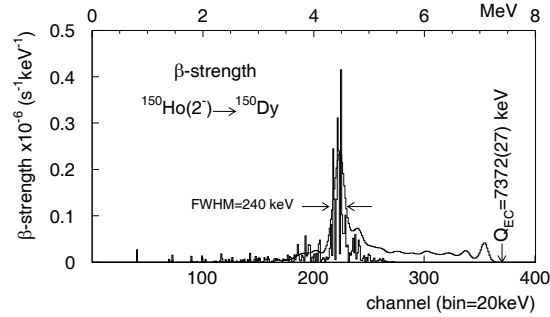


Fig. 6 – The beta strength as a function of excitation energy in the daughter nucleus following the beta decay of ^{150}Ho measured with the CLUSTER CUBE (sharp lines) and the GSI TAS (continuous function) (see text).

results we should mention that 1 064 gamma-ray lines were observed, which were arranged into a decay scheme with 295 levels in ^{150}Dy . On the assumption that the beta decays are allowed GT decays it was possible to assign spins and parities to most of them.

In this study Shell model analysis provides a prediction of the distribution of $B(\text{GT})$ strength between the 1^- , 2^- and 3^- states of 3.6:4.0:7.4 normalised to 15 arbitrary units. This is in excellent agreement with the measured ratios of 3.4:4.2:7.4 (now in units of $g_A^2/4\pi$) derived from the CLUSTER CUBE measurements.

In Fig. 6 one can see clearly the most distinctive feature of the spectra from both types of spectrometer, namely the very strong beta feeding to a narrow interval near 4.4 MeV with a width of about 240 keV. This corresponds to the $\pi h_{11/2}$ to $\nu h_{9/2}$ transition we anticipated seeing earlier. This is the peak of the GT resonance, more or less at the energy anticipated. The two spectra have the same shape, which gives confidence in the analysis techniques used for the TagS spectrum. There is, however, a clear loss in sensitivity in the CLUSTER CUBE spectrum at higher energies. Quantitatively we can say that the total $B(\text{GT})$ up to the highest observed level at 5.9 MeV is 0.267 corresponding to $\log ft = 4.16$. This compares with values of 0.455 and 3.93 obtained for these quantities from the TAgS up to the same energy. If we take the total $B(\text{GT})$ up to the Q_β window then we miss, in total, 50% of the $B(\text{GT})$ in this very high quality Ge measurement. On the other hand the individual levels and gamma transitions can only be disentangled in the spectra from the Ge detector array. This is shown qualitatively in Fig. 7, where the region of the resonance measured with the GSI TAS is compared with the spectra from some coincidence gates showing gammas de-exciting levels in the same region.

What can we conclude from these studies? Firstly it demonstrates very clearly and beautifully the population of the GT resonance in beta decay within the Q_β window. Secondly it demonstrates the clear need for the use of both techniques in such cases. The TAgS measurements are essential because it is the only way to obtain a proper measure of the GT decay strength. The high resolution measurements are also essential if one wants the details of the daughter level scheme and the fine structure of the resonance.

4.2. MEASUREMENT OF NUCLEAR SHAPES IN BETA DECAY

The shape of the nucleus is one of the simplest of its macroscopic nuclear properties to visualise. In practice it turns out to be very difficult to measure. As we shall see below it turns out [12] that, in some cases, one can determine the nuclear shape including its sign from studies of beta decay. In general terms

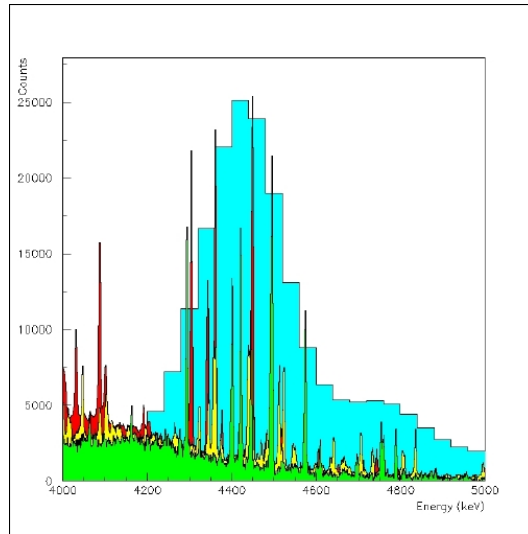


Fig. 7 – Comparison of part of the GSI TAS and CLUSTER CUBE spectra (various coincidence gates) for the decay of the 2^- ground state in ^{150}Ho (see text).

we now have a picture of nuclei at closed shells having spherical shapes and nuclei with even quite small numbers of valence nucleons being deformed. The nuclei with $A \sim 70 - 80$ and $N \sim Z$ are of particular interest in this context. These nuclei enjoy a particular symmetry since the neutrons and protons are filling the same orbits. This, together with a low single-particle level density, leads to rapid changes in deformation with the addition or subtraction of only a few nucleons. In terms of mean field models, these rapid changes occur because of the proximity in energy of large energy gaps for protons and neutrons at $Z, N = 34, 36$ on the oblate side and $Z, N = 38$ on the prolate side of the Nilsson diagram. Such models suggest [32, 33] the co-existence of states in these nuclei of quite different shape. There is experimental evidence to support this in the Se and Kr nuclei [34, 35] and it is also predicted for the lightest Sr nuclei.

As a result it is of considerable interest to map out the deformation of both the ground and excited states in these nuclei. In practice, this is not a simple task. There are a number of methods of measuring the ground state deformation in unstable nuclei based on the interaction of the electric quadrupole moment of the nucleus with an external electric field gradient [36, 37]. However these methods do not apply to nuclei with $J = 0$ or $1/2$. Apart from the nuclear re-orientation effect in Coulomb excitation, however, they do not give the sign of the quadrupole moment and thus cannot distinguish between oblate and prolate shapes.

In some cases beta decay provides an alternative way of deducing whether the ground state of the parent nucleus is oblate or prolate. The basis of the method is an accurate measurement of the Gamow-Teller strength distribution, $B(\text{GT})$, as a function of excitation energy in the daughter nucleus. The idea was first put forward by Hamamoto *et al.* [38] and was then pursued in in more detail by Sarriguren *et al.* [39]. In essence they calculate the $B(\text{GT})$ distributions for various nuclei in the region for the deformations minimising the ground state energy. In some cases the calculated distributions within the beta decay window differ markedly with the shape of the ground state of the parent nucleus, especially for the light Kr and Sr isotopes.

A number of cases have been studied with the *Lucrecia* spectrometer described earlier. In the case of the even-even nucleus ^{76}Sr it was already known that the ground state is amongst the most deformed known. This was based on the measurement [40] of the energy of the first excited 2^+ state and Grodzin's formula [41], an empirical relationship between the deformation and the energy of the $2^+ - 0^+$ transition. This tells us nothing about the sign of the deformation.

CERN-ISOLDE is, at present, the ideal place for measuring the beta decay of ^{76}Sr , since it provides the most intense, mass-separated, low-energy beams of neutron-deficient Sr nuclei. The half life of ^{76}Sr is just 8.9 s. This is long enough for us to be able to implant the activity on the tape outside the shielding for *Lucrecia* and then transport it to the counting point. The tape system was moved every 15s in order to avoid the buildup of the ^{76}Rb daughter activity, which has a half-life of 36.8 s. The gamma-ray spectrum was recorded in coincidence with positrons and X-rays using the ancillary detectors placed close to the implanted source in the central through hole in the NaI detector. The upper part of Fig. 8 shows the experimental total absorption spectrum of the beta decay of ^{76}Sr overlaid with the recalculated spectrum after the analysis. In the lower panel we see the $B(\text{GT})$ distribution derived from this spectrum with the shading indicating the experimental uncertainty. These results were based on the singles spectra and did not use the recorded coincidences.

The reader should note a number of points. Firstly the analysis of the TAgS spectrum was carried out as outlined in Section 3.2. Secondly the proton separation energy is 3.5 MeV. As a result beta-delayed proton emission has been observed at excitation energies from 4.8–5.8 MeV [42]. However, this contribution is only $\sim 2\%$ in $B(\text{GT})$, i.e. very small compared to decay *via* beta-delayed gamma rays. Thirdly the marked strength at 0.5, 1.0 and 2.1 MeV is to states already known [43] but the $B(\text{GT})$ values reported earlier are in disagreement with the TAgS measurements as a result of the ‘‘Pandemonium’’ effect described above.

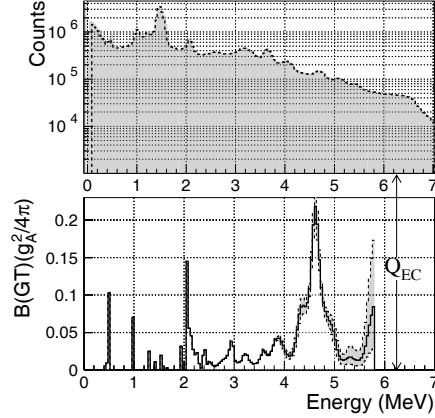


Fig. 8 – The upper part of the figure shows the singles spectrum overlaid with the spectrum recalculated after analysis. The lower part shows the $B(\text{GT})$ distribution as a function of excitation energy in the daughter nucleus. The shading indicates the experimental uncertainty.

The theoretical derivation [39] of the $B(\text{GT})$ distribution starts with the construction of the quasi-particle basis self-consistently from a deformed Hartree-Fock (HF) calculation with density dependent Skyrme forces and pairing correlations in the BCS framework. From the minima in the total HF energy *versus* deformation plot they derive the possible ground state deformations. In the case of ^{76}Sr two minima are found; one is prolate with $\beta_2 = 0.41$, the other is oblate with $\beta_2 = -0.13$. Using these results the quasi-random-phase approximation (QRPA) equations are solved with the interaction derived from the same Skyrme force used in the HF calculation. To calculate the $B(\text{GT})$ it is assumed that the states populated in the daughter nucleus have the same deformation as the parent state.

Figure 9 shows the results of these calculations using the SK3 residual interaction. This plot shows the sum of the $B(\text{GT})$ at any given energy bin up to that energy bin. The theoretical results are shown for both prolate and oblate states. It also shows the measured, accumulated $B(\text{GT})$. The shading indicates the experimental uncertainty. The agreement of the experimental plot with the calculation for a prolate shape is very good over the energy range 0–5 to 6 MeV. In contrast there is no agreement with the results of the calculation based on an oblate shape. Thus our results confirm the large deformation, $\beta_2 \sim 0.4$, deduced from the in-beam studies and give the first definitive evidence that the deformation is of prolate character.

This result also validates this method of determining the ground state deformation. It was also applied to the case of ^{74}Kr [13], where earlier measurements [35] of the decay of the isomeric, first excited 0^+ state had indicated

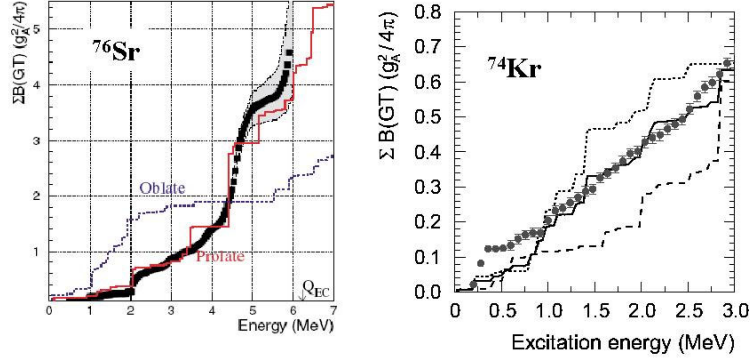


Fig. 9 – On the left hand side we see the summed value of the measured $B(\text{GT})$ as a function of the excitation energy in the daughter nucleus for the decay of ^{76}Sr [12] compared with the theoretical distributions for oblate and prolate shapes. On the right we see the the same thing for ^{74}Kr .

strong mixing of the oblate and prolate shapes. Again the TAGS measurements were made at CERN-ISOLDE. Figure 9 also shows the accumulated $B(\text{GT})$ as a function of excitation energy for both theory and experiment. This time it is clear that there is a mixture of prolate and oblate shapes in the ^{74}Kr ground state. This is confirmed by the Coulomb excitation of a beam of ^{74}Kr [44].

Summarising, it is clear that it is possible, in some cases, where there is sufficient difference between the calculated curves, to determine the shape of the nuclear ground state from measurements of the $B(\text{GT})$ distribution. As part of the same programme of measurements a number of other Kr and Sr decays were also studied. The results will appear in due course.

5. FUTURE MEASUREMENTS

One of the most important changes in studies of nuclear physics in recent years has been the steady development in our ability to accelerate radioactive nuclear species. This has allowed us and will continue to allow us to study the beta decay of more and more exotic nuclear species. As we have explained above, if we are to extract the fullest information from these studies we must use both the high resolution and total absorption techniques. At the new international radioactive beam facilities FAIR, to be built at GSI, Darmstadt, and SPIRAL2, to be built at GANIL, France, plans are already underway [45, 46] to allow both types of study and also to allow studies of beta-delayed neutrons as well.

In the operation of nuclear reactors based on thermal neutron-induced fission seven percent of the total power comes from radioactive decay. When the reactor shuts down this activity dies away over a long period. In order to be able to optimise reactor operation and calculate properly the shielding needed for radioactive waste we need a precise knowledge of the cooling curve. This requires a knowledge of the decays of a large number of beta decays. In particular it is essential to have a proper knowledge of the beta-feeding distribution for these decays. Many of these have been inaccessible to study until now because it has been impossible to separate chemical species which are refractory. New types of ion source [47] and the IGISOL technique [48] now allow us to separate such species and the required measurements are now planned [49]. Initial studies of Tc isotopes have been undertaken at the IGISOL at Jyväskylä [50] and it is clear that the results greatly improve the calculated decay heat curves.

Acknowledgements. This article was written as part of a volume to celebrate the work and achievements of Professor Dorin Poenaru on the occasion of his 70th birthday. Amongst his many works and achievements were important contributions to our understanding of radioactive decay. In particular the prediction that radioactive decay might occur by the emission of ^{14}C . We felt that our article on beta decay would be a fitting measure of our esteem.

This work was partly supported by the grant FPA2005-03993 of the Spanish Ministry of Education and Research.

REFERENCES

1. S. Hofmann, *On beyond Uranium Science Spectra*, ed. by V. Moses, London, Taylor and Francis, 2002.
2. M. Jung *et al.*, Phys. Rev. Lett., **C 77**, 5190 (1996).
3. F. Bosch *et al.*, Phys. Rev. Lett., **C 69**, 2164 (1992).
4. M.V. Stoitsov *et al.*, Phys. Rev., **C 68**, 054312 (2003).
5. W. Pauli, *Rapports du Septieme Conseil de Physique Solway*, Brussels, 1933.
6. E. Fermi, Z. Phys., **88**, 161 (1934).
7. Z. Hu *et al.*, Phys. Rev., **C 60**, 024315 (1999); *ibid.*, **62**, 064315 (2000); M. Gierlik *et al.*, Nucl. Phys., **A 724**, 313 (2003).
8. P. Kleinheinz *et al.*, Phys. Rev. Lett., **55**, 2664 (1985).
9. A. Algora *et al.*, Phys. Rev., **C 68**, 034301 (2003).
10. B. Rubio, *Frontiers of Collective Motions* (CM2002), ed. by H. Sagawa and H. Iwasaki, Singapore, World Scientific, 2002.
11. E. Nacher *et al.*, GSI Sci. Report, p. 8; <http://www-aix.gsi.de/annrep2002/Files/8.pdf>, 2003.
12. E. Nacher *et al.*, Phys. Rev. Lett., **92**, 232501 (2004).
13. E. Poirier *et al.*, Phys. Rev., **C 69**, 034307 (2004).
14. J.C. Hardy *et al.*, Nucl. Phys., **A 509**, 429 (1990).

15. I.S. Towner and J.C. Hardy, Proc. of Vth Int. Wein Symposium: *Physics beyond the Standard Model*, Santa Fe, NM, June 1998, ed. by P. Herczeg, C.M. Hoffmann and H.V. Klapdor-Kleingrothaus, World Scientific, Singapore, 1999, p. 338.
16. J.C. Hardy and I.S. Towner, Phys. Rev. Lett., **94**, 09250 (2005).
17. W. Gelletly and J. Eberth, *The Euroschool Lectures on Physics with Exotic Beams*, Vol. II, J. Al-Khalili and E. Roeckl eds., Springer, Berlin, Heidelberg, New York, 2006, p. 79.
18. J.C. Hardy *et al.*, Phys. Lett., **B 71**, 307 (1977).
19. C.L. Duke *et al.*, Nucl. Phys., **A 151**, 609 (1970).
20. K.H. Johansen *et al.*, Nucl. Phys., **A 203**, 481 (1973).
21. R.B. Firestone *et al.*, Phys. Rev., **C 25**, 527 (1982).
22. Alkhazov *et al.*, Phys. Lett., **B 157**, 35 (1985).
23. R.C. Greenwood *et al.*, Nucl. Inst. Meth., **A 314**, 514 (1992).
24. J.L. Tain and D. Cano-Ott, Nucl. Inst. Meth., **A 571**, 719 (2007).
25. J.L. Tain and D. Cano-Ott, Nucl. Inst. Meth., **A 571**, 728 (2007).
26. D. Cano-Ott, Ph.D. Thesis, University of Valencia, 2002.
27. A. Perez and B. Rubio, private communication.
28. M.Karny *et al.*, Nucl. Inst. Meth., **B 126**, 411 (1997).
29. D. Cano-Ott *et al.*, Nucl. Inst. Meth., **A 430**, 333 (1999).
30. D. Cano-Ott *et al.*, Nucl. Inst. Meth., **A 430**, 488 (1999).
31. J. Eberth *et al.*, Nucl. Inst. Meth., **A 369**, 135 (1996).
32. W. Nazarewicz *et al.*, Nucl. Phys., **A 435**, 397 (1985).
33. P. Bonche *et al.*, Nucl. Phys., **A 443**, 39 (1985).
34. J.H. Hamilton *et al.*, Phys. Rev. Lett., **32**, 239 (1974).
35. C. Chandler *et al.*, Phys. Rev., **C 56**, R2924 (1997).
36. E. Davni *et al.*, Phys. Rev. Lett., **50**, 1652 (1983).
37. F. Hardeman *et al.*, Phys. Rev., **C 43**, 130 (1991).
38. I. Hamamoto *et al.*, Z. Phys., **A 353**, 145 (1995).
39. P. Sarriguren *et al.*, Nucl. Phys., **A 691**, 631 (2001).
40. C.J. Lister *et al.*, Phys. Rev., **C 42**, R1191 (1990).
41. L. Grodzins, Phys. Lett., **2**, 88 (1966).
42. Ch. Miede *et al.*, in *New Facet of Spin Giant Resonances in Nuclei*, ed. by H. Sakai, 1997, p. 140.
43. Ph. Dessagne *et al.*, Eur. Phys. J., **A 20**, 405 (2004).
44. W. Korten *et al.*, Nucl. Phys., **746**, 90c (2004).
45. B. Rubio, Int. J. Modern Phys., **15**, 1979 (2006).
46. ***, [http://www.ganil.fr/research/developments/spiral2/files/ LoIs SP2 final/LoI SP2 1 DESIR final.pdf](http://www.ganil.fr/research/developments/spiral2/files/LoIs%20SP2%20final/LoI%20SP2%201%20DESIR%20final.pdf).
47. V.N. Fedoseyev *et al.*, Nucl. Inst. Meth., **B 126**, 88 (1997).
48. J. Aysto, Nucl. Phys., **A 693**, 477 (2001).
49. J.L. Tain and A. Algora, private communication.
50. A. Algora *et al.*, to be published.